Structural and Dispersion Parameters of PVA-PAAm-CuNW for Optical and antibacterial applications

Zainab Mohammed Jawad[1] Khalid Haneen Abass[2]
[1,2]Department of Physics, College of Education for Pure Sciences University of Babylon, Iraq
zainab.mohammed.pure309@student.uobabylon.edu.iq,
pure.khalid.haneen@uobabylon.edu.iq

Abstract

The PVA-PAAm-CuNW nanocomposites were prepared by casting method at thicknesses (90) µm with different weight percentages (0.5, 1, 2 %.wt) of CuNW additives at a temperature of 70 oC. The structural, optical properties, and dispersion parameters of nanocomposites were studied. The results of the optical microscopy photos show good distribution of CuNW inside the polymer blends of the nanocomposite films. According to scanning electron microscopy (SEM), the surface of PVA-PAAm-CuNW nanocomposites had a homogeneous morphology that revealed a relatively soft surface. However, as the ratio of CuNW in the polymer matrix increased, the surface's morphology changed and its roughness increased. The results of the FTIR spectrum of the nanostructure showed that all the peaks, not most of the absorbance bonds, remain at the same location of the wavenumber, refer to no chemical reaction occurred between the PVA-PAAm and CuNW, while the chemical reaction accrued between the PVA and PAAm polymers. The results of the optical properties of PVA-PAAm-CuNW nanocomposites showed that the refractive index, absorption coefficient increase with the increases the concentrations of CuNW, while the transmittance and energy gap decreased. The dispersion parameters such as; Eo, Ed, no, εα, M−1, M−3 were calculated using the Wemple–DiDomenico model. The value of the energy gap estimated by Wemple–DiDomenico calculations was consistent with the value of the optical energy gap obtained from Tauc relation. From the studied properties, the prepared films were suitable for optical devices and antibacterial application.

Keywords: PVA-PAAm-CuNW, Nanocomposite, optical properties, Scanning electron microscope, Dispersion parameters.

1. Introduction

Polymer composites have received a lot of interest in the past 10 years because of the potential applications they could have in many different fields. Polymers have garnered this level of attention due of their alluring properties, such as flexibility, abundance, and low cost [1-3]. Additionally, their ability to change their properties makes them suitable for use in a variety of applications. This objective can be accomplished either by combining numerous homopolymers or by filling them with specific substances to match certain applications. These include uses in optoelectronics, solar energy, shielding, energy storage, biotechnology, and medicine [4, 5]. Poly (vinyl alcohol) (PVA) has been the focus of numerous investigations due to their stimulating qualities. In addition to optical properties, this material also possesses a high charge-storing capacity, low cost, good mechanical and commercial availability, and a high dielectric strength [6]. Numerous researchers have studied the use of PVA as fillers or in cross-linked goods, and it has also been extensively used in nontoxic, safe, living tissues, etc [7, 8]. Polyacrylamide (PAAm) is an additional water-soluble polymer with a variety of industrial applications [9]. The applications may be advantageous due to the weak tensile strength, poor pressure resistance, and absence of lengthening [10]. The Copper Nanowire (CuNW) have been examined through numerous intensive researches that have led to the discovery of their use in many scientific, and industrial fields. the Cu nanomaterials exhibited unique properties, containing thermal, optics, mechanics [11]. Cu NW films can achieve high optical transmittance with high electric conductivity [12, 13].
The aims work, preparation of (PVA-PAAm-CuNW) nanocomposite by using casting method and investigate structural, Optical Properties and Dispersion Parameters.

2. Materials and Methods

2.1 Matrix material

Polyvinyl Alcohol (PVA)

The polymer was used as granular form, (PVA) was supplied from (Panreac\Spain, Lnc) Barcelona Espana (M.W = 18000-12000), with high purity (99.0%)

Poly Acrylamide (PAAm)

The polymer was used in a white granular form soluble in water, and Its molecular weight was (5×106 g/mol), with high purity (99.99 %). It is manufactured by a company (British Drug Houses (BDH)).

2.2 Additive nanomaterial

Copper Nanowire (CuNW)

Copper Nanowire supplier Houston USA, (Purity 99.5%, Diameter 100 nm, Length 10 µm).

2.Methods

Polymers nanocomposites films have been made by combining 80% PVA in 50 mL of distilled water, in a glass beaker equipped with a magnetic stirrer, the mixing

doi.org/10.31838/hiv22.02.164 Received: 08.06.22, Revised: 09.06.22, Accepted: 18.08.22

process proceeded for 30 min to obtain more uniform solution with temperature of 70 oC. Then 20% PAAm was added to the mixture under continuous stirring for 1h to get a mixture of more homogenous solution with temperature of 70 oC. Then the temperature of the PVA-PAAm matrix was reduced to about 40 ºC before adding three ratios (0.5, 1, 2) wt.% of CuNW for 1 h of each case to prepare PVA-PAAm-CuNW nanocomposite films as shown in Table (1). Then the mixture was left in the glass beaker for 24 hours. Each one of these ratios has been casted in a petri dish (9 cm in diameter). The entire set is placed in a dust-free room and the solvent is allowed to slowly evaporate into air at room temperature for 7 days. Then it is peeled of the petri dish gently. The thickness of these films was measured and found to be within (90) µm. The steps of the composite preparation are shown in Figure (1).

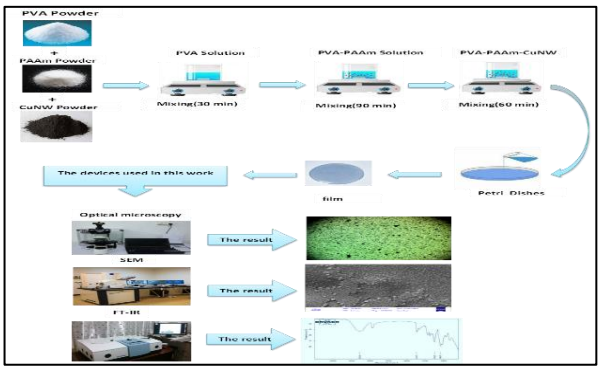

Figure (1): The practical diagram.

Table (1): Weight percentages of PVA-PAAm-CuNW Nanocomposites.

PVA (gm)	PAAm (gm)	CuNW (gm)
0.8	0.2	0.0
0.796	0.199	0.005
0.792	0.198	0.01
0.784	0.196	0.02

3. Results and Discussion

3.1 Optical Microscopy (OM)

The morphological properties of the films have been showed using OM at magnification power (100x). Figure (2) show the images of PVA-PAAm-CuNW nanocomposites with concentrations of CuNW. These pictures showed how evenly distributed CuNW was throughout the blend-polymer composites, along with good matrix homogeneity. The PVA-PAAm-CuNW nanocomposites were successfully synthesized using this technique, as shown by the OM pictures. In compared to the polymers blending films, the PVA-PAAm-CuNW nanocomposites films exhibited a significant change as the CuNW ratio was increased. The contribution of CuNW revealed numerous alterations in all of these films without affecting their transparency. In addition, raising the ratio of CuNW significantly improved the fine dispersion, as shown in Figure (2.d). The results agree with the results of the previous researchers [14].

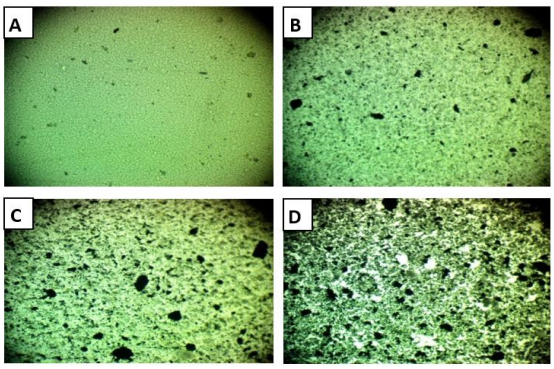

Figure (2): Photomicrographs of PVA-PAAm at 100X magnifications with varying CuNW contents: (A) 0%, (B) 0.5%, (C) 1%, and (D) 2%.

3.2 Scanning electron microscopy (SEM)

Scanning electron microscopy was used to analyze the surface morphology of the samples and the distribution of CuNW within the polymer matrix. A SEM image of the surface of films made of PVA-PAAm and PVA-PAAm-CuNW nanocomposites is shown in Figure 3. The consistent morphology in figure (3)'s photos (A, B) reveals a relatively soft surface. The PVA-PAAm-CuNW nanocomposites in figure (3) (C and D) changed in surface morphology and roughness due to an increase in the ratio of CuNW in a polymer matrix. The nanocomposite films exhibit numerous CuNW that were finely dispersed without aggregates and scattered widely throughout the surface, which may be an indication of the occurrence of a homogenous growth mechanism. The findings concur with those of earlier researchers.

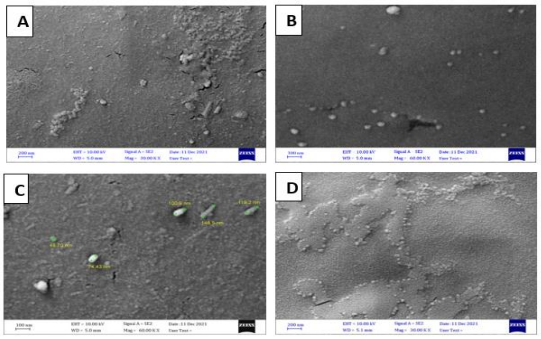

Figure (3): SEM images of PVA-PAAm with various content of CuNW: (A) 0 wt.% (B) 0.5 wt.% (C) 1 wt.% and (D) 2 wt.%.

3.2 Fourier transform infrared rays (FTIR)

As shown in Figure 4, the FTIR spectra of PVA-PAAm-CuNW nanocomposites with varied CuNW ratios and thicknesses were acquired at room temperature in the range (4000-500 cm-1). The functional groups generated in composites showed distinctive regions of stretching and bending vibrations in the spectra. From these spectra it can be noted that the absorption peaks at about (3280.51, 3285.54, and 3275.87) cm-1 were attributed assigned to the stretching vibration of hydroxyl group (OH) in the polymer matrix chain [15]. As for the absorption peak at (2937.32) cm-1 were attributed to methylene (C-H) stretching while the band (1732.75) cm-1 were attributed to carboxyl acid (C=O) stretching [16]. Meanwhile, the functional groups at (1238.76, 1240.27)

cm-1 of all them attributed to carbon dioxide (C-O) stretching [17]. At (1084.75) cm-1, the peak is recognized as (C-C) stretching vibration [18]. FTIR spectra shows a shift in peak position as well as the change in shape and intensity comparing with pure PVA-PAAm films also it can be noticed that the peak at 3300 cm-1 which belong to PVA polymer and represent the (OH) stretching vibration bond, did not appear in these peaks, while the peaks (3280.51, 3285.54, and 3275.87) cm-1 that belonged to (OH) stretching vibration appeared. As well the peak at 1141 cm-1 which belong to PVA polymer and represent the C-O stretching bond, while the peak 1323 cm-1 that belongs to PAAm polymer did not appear in these peaks. Instead the peaks (1238.76, 1240.27) cm-1 that associated with C-O stretching appeared. There is a simple shift in the (C-H) stretching bond which represent PVA and PAAm polymer, that move and become at 2937.32 cm-1, instead of the 2940 cm-1 and 2931 bond for the same polymer which also goes back to (C-H) stretching. As well there is a simple shift in the (C=O) stretching bond, which represent PVA polymer that move and become at 1732.75 cm-1 instead of the 1731 cm-1 bond for the same polymer which also goes back to (C=O) stretching, and there is a simple shift in the (C-C) stretching bond which represent PVA polymer that move and become at 1084.75 cm-1 rather than the 1087 cm-1 bond for the same polymer which also goes back to (C-C) stretching [19, 20]. Additionally, it is apparent that the transmittance decreases as the amount of CuNW rises. As seen in figures (4) as in the images (B, C and D), the increased film density results in more atoms and ions in the light path as well as enhanced UV and IR absorption. The findings concur with those of earlier researchers [21].

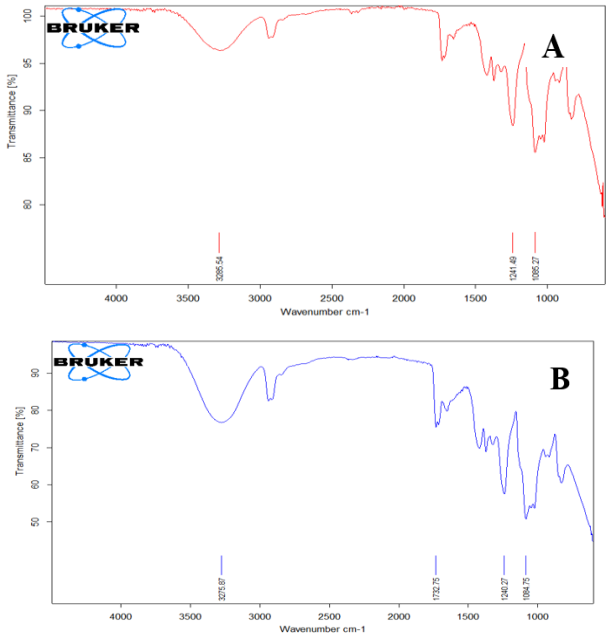

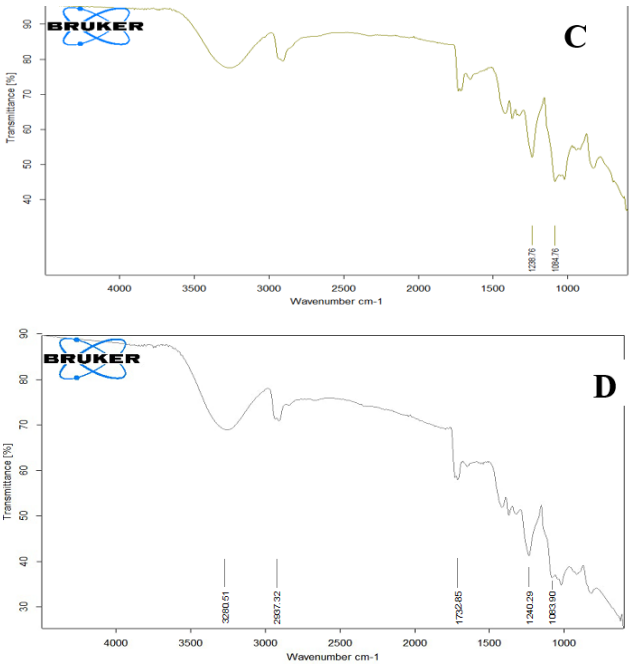

Figure (4): FTIR spectra of PVA-PAAm with varying concentrations of CuNW are shown in (A) 0 wt%, (B) 0.5 wt%, (C) 1 wt%, and (D) 2 wt%.

3.3 Optical Properties

The transmittance (T) was calculated utilizing equation (1). Figure 5 depicts the transmittance spectrum of PVA-PAAm-CuNW nanocomposites as a function of wavelength. It can be observed that the transmittance increases with increasing wavelength and decreases with increasing CuNW content. This has been made possible by the addition of CuNW, which contains electrons with the ability to absorb electromagnetic energy and move to a higher level. Because there are no particles on (pure) film, it has a high transmittance. Since there aren't any free electrons present, it takes a lot of energy to transition and break the bonds. The findings concur with those of earlier researchers [22].

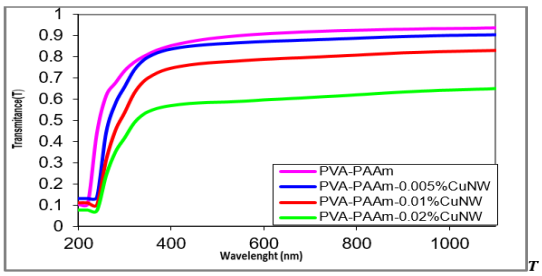

$$T = \frac{I_T}{I_o} \quad (1)$$

Figure (5): Transmission of PVA-PAAm Blend and PVA-PAAm-CuNW Nanocomposites as a function of wavelength.

The refractive index was calculated utilizing equation (2). The variation of the index of refraction of PVA-PAAm-CuNW nanocomposites as a function of wavelength is depicted in Figure 6. The graphs demonstrate that the refractive index increases with increasing weight percent CuNW concentration in polymers and decreases with increasing wavelength. This tendency is related to the rise in the density of nanocomposites. The refractive index values will rise when incident light interacts with a sample that has a high refractive index in the UV region. The

findings concur with those of earlier researchers [23].

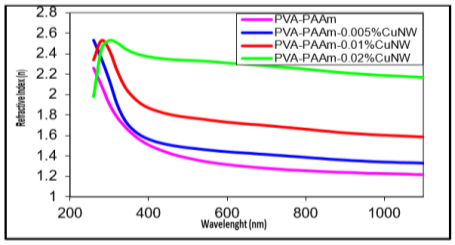

$$n = \sqrt{\frac{4R - k^2}{(R-1)^2}} - \frac{(R+1)}{(R-1)} \quad (2)$$

Figure (6): The refractive index (n) of PVA-PAAm Blend and PVA-PAAm-CuNW Nanocomposites as a function of wavelength.

The absorption coefficient (α) was calculated utilizing equation (3). Figure 7 depicts the absorption coefficient (α) of PVA-PAAm-CuNW nanocomposites as a function of wavelength. The energy of the input photon is insufficient to shift the electron from the valence band to the conduction band, which causes the absorption coefficient to be lowest at long wavelengths (low energy), suggesting a low chance of electron transition. The energy of the input photon is sufficient to transfer one electron from the valence band to the conduction band since absorption increases at high energies, indicating a high likelihood for electron transitions. The energy of the input photon exceeds the forbidden energy gap, indicating that the absorption coefficient helps determine the kind of electron transition at high energies (α>104 cm-1) when the absorption coefficient values are large. It is anticipated that direct electron transition would occur, with electrons and photons maintaining their energy and momentum. Whereas, when the absorption coefficient is low (α<104 cm-1) at low energies, it is envisaged that indirect electron transition will occur and the electronic momentum will be maintained with the aid of the phonon. The findings concur with those of earlier researchers [24].

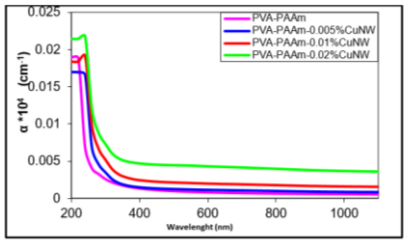

$$\alpha = 2.303 \left(\frac{A}{t}\right) \quad (3)$$

Figure (7): The absorption coefficient spectra of PVA-PAAm Blend and PVA PAAm-CuNW Nanocomposites as a function of wavelength.

Equation (4) has been used to determine the allowed and forbidden indirect transition band energy gaps. The permitted indirect transition band gap was calculated when r = 2, whereas the prohibited indirect transition band gap was established when r = 3. Figure 8 shows the correlation between the photon energy and the absorption edge (hv)1/2 for PVA-PAAm-CuNW nanocomposites. We can determine the energy gap for the permitted indirect transition by drawing a straight line from the curve's top region to the (x) axis at the value (hv)1/2=0 [25].

The table displays the results (2). It is evident that the values of the energy gap decline as the weight percentages of CuNW rise. By increasing the CuNW weight percent, the transition in this sample took place in two stages and entailed the transfer of electrons from the valence band to the local levels to the conduction band. This was attributed to the production of site levels in the forbidden energy gap. This behavior was attributed to the heterogeneous nature of nanocomposites (i.e., the dependence of the electronic conduction on the addition of materials). The decrease in energy gap with increasing CuNW is due to the development of electronic pathways by CuNW in the polymer that make it easier for electrons to move from the valance band to the conduction band. The findings concur with those of earlier researchers [26].

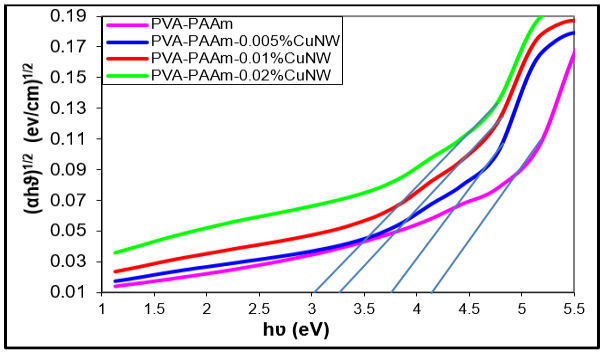

$$\alpha h\upsilon = B(h\upsilon - E_g{}^{opt} \pm E_{ph})^r \quad (4)$$

Figure (8): Plots of $(\alpha h\upsilon)^{1/2}$ vs photon energy (hv) for PVA-PAAm-CuNW Nanocomposites, respectively.

3.4 Dispersion Parameters

Dispersion parameters are critical in many applications, including optical communication and optical device design. These parameters were introduced by Wemple–DiDomenico according to the following equation [27]:

$$(n^2 - 1) = \frac{E_d E_0}{E_0{}^2 - (h\upsilon)^2} \quad (5)$$

Where n is the refractive index, Ed represents the dispersion energy, while Eo is the single oscillator energy of the electronic transitions. A plot of (n2 - 1)-1 against (hv)2, was used to estimate Eo and Ed which were calculated from the slope (Eo Ed) -1and intercept (Eo / Ed). The calculated values were listed in Table 3 showing at films with a thickness of 90 µm, we can see that as CuNW increases, Eo and Eg decrease, while the other parameters increase. The value of the average energy gap can be calculated from the energy of the simple oscillator by the approximation relation(Eo ≈ 2Eg). The value of the energy gap estimated by Wemple–DiDomenico was in agreement with the value derived from the Tauc relation. The static refractive index (no) and static dielectric constant can be calculated using the following relations [28]

$$n2(0) = 1 + \frac{E_d}{E_0} \quad (6)$$

$$\varepsilon_\infty = n2(0) \quad (7)$$

The following equations can be used to compute the moments of the imaginary component of the optical spectrum M-1 and M-3 of CuNW thin films [29, 30]:

$$E_0^2 = \frac{M_{-1}}{M_{-3}} \quad (8)$$

$$E_d^2 = \frac{M^3{}_{-1}}{M_{-3}} \quad (9)$$

Table (2): The values of the allowable indirect transition energy gap of PVA-PAAm-CuNW nanocomposites with a thickness of 90 µm.		
Samples	Allowed indirect transition (eV)	
	thickness of 120 µm	thickness of 90 µm.
PVA-PAAm	4.10	4.12
PVA-PAAm-0.5%CuNW	3.70	3.75
PVA-PAAm-1.0%CuNW	3.25	3.27
PVA-PAAm-2.0%CuNW	3.00	3.00

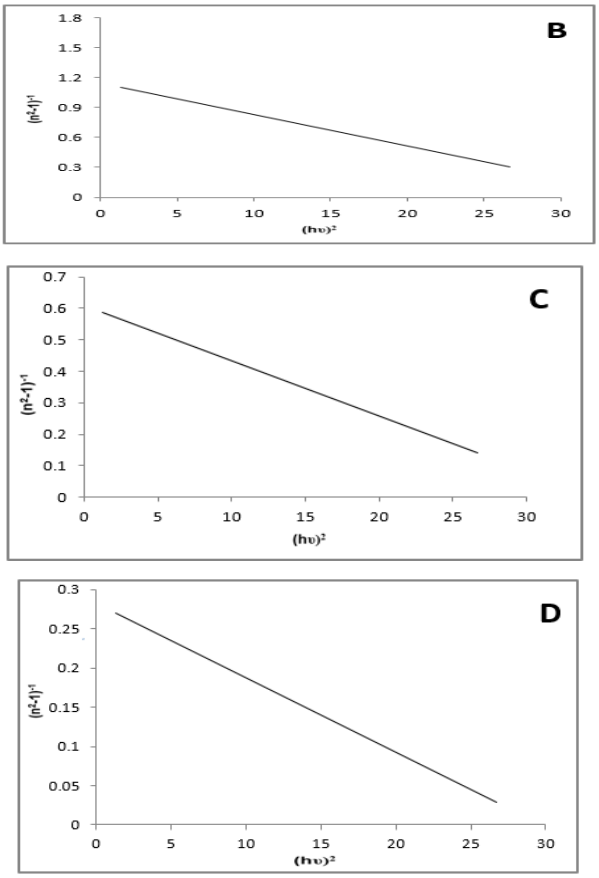

Figure(9): Plot of (n2 -1)-1 vs (hυ)2 of PVA-PAAm with various content of CuNW: (A) 0 wt.% (B) 0.5 wt.% (C) 1 wt.% and (D) 2 wt.%.

Table(3): Dispersion parameters of PVA-PAAm-CuNW Nanocomposites.				
parameter	PVA-PAAm			
	0.0	0.5 wt.% CuNW	1.0 wt.% CuNW	2.0 wt.% CuNW
Eo	7.91	5..96	5.80	5.50
Ed	4..85	5.18	9.51	19.66
Eg	3.95	2.98	2.90	2.57
n2(0)	1.61	1.86	2.63	4.57
no(0)	1.27	1.36	1.62	2.13
ε	1.61	1.86	2.63	4.57
M-1	0.61	0.86	1.63	3.57
M-3	0.009	0.02	0.04	0.01

4. Conclusions

It was found through the study that the PVA-PAAm-CuNW composite appears a continuous change in its physical properties (structural, optical, and dispersion parameters) as a result of CuNW additive. Optical microscopy and Scanning Electron Microscopy data demonstrate that the utilized technique successfully produced novel nanocomposites with homogeneous and fine dispersion. The films have a homogeneous morphology that reveals a relatively soft surface. We conclude that increasing the CuNW ratio in a polymer matrix for PVA-PAAm-CuNW nanocomposites caused changes in surface morphology and increased roughness. The FTIR spectra show a shift in some bands and change in the intensities of other bands compared to the PVA-PAAm-CuNW nanocomposite films. The decrease in transparency can also be observed with an increase in the CuNW. The indices of refraction and absorption coefficient of PVA-PAAm-CuNW nanocomposites increase as CuNW concentration rises, while the transmittance and energy gap of indirect transition (allowed) decreased. From the Wemple–DiDomenico model, the dispersion parameters were determined. The value of the energy gap obtained from Wemple–DiDomenico was comparable with the value of the optical energy gap obtained from Tauc relation. From the studied properties, the prepared films were suitable for optical devices, solar cell and antibacterial application.

References

1. Badawi A. Engineering the optical properties of PVA/PVP polymeric blend in situ using tin sulfide for optoelectronics. Applied Physics A. 2020;126(5):1-12. https://doi.org/10.1007/s00339-020-03514-5

2. Abass KH, Kadim AM, Mohammed SK, Agam MA. Drug Delivery Systems Based on Polymeric Blend: A Review. Nano Biomed Eng. 2021;13(4):414-24. Available from: https://www.researchgate.net/publication/357880939

3. Dhatarwal P, Sengwa R. Investigation on the optical properties of (PVP/PVA)/Al2O3 nanocomposite films for green disposable optoelectronics. Physica B: Condensed Matter. 2021;613:412989. https://doi.org/10.1016/j.physb.2021.412989

4. Khairy Y, Mohammed M, Elsaeedy H, Yahia I. Optical and electrical properties of SnBr2-doped polyvinyl alcohol (PVA) polymeric solid electrolyte for electronic and optoelectronic applications. Optik. 2021;228:166129. https://doi.org/10.1016/j.ijleo.2020.166129

5. Xu F, Yang Y, Liu Y, Yang J, Liao Y, Wang X, Shi X, Hu J. Ferrite ceramic filled poly-dimethylsiloxane composite with enhanced magnetic-dielectric properties as substrate material for flexible electronics. Ceramics International. 2021;47(13):18246-51. https://doi.org/10.1016/j.ceramint.2021.03.144

6. Hdidar M, Chouikhi S, Fattoum A, Arous M, Kallel A. Influence of TiO2 rutile doping on the thermal and dielectric properties of nanocomposite films based PVA. Journal of Alloys and Compounds. 2018;750:375-83. https://doi.org/10.1016/j.jallcom.2018.03.272

7. Qiu K, Netravali AN. Fabrication and characterization of biodegradable composites based on microfibrillated cellulose and polyvinyl alcohol. Composites Science and Technology. 2012;72(13):1588-94. https://doi.org/10.1016/j.compscitech.2012.06.010

8. Qiu K, Netravali AN. A composting study of membrane-like polyvinyl alcohol based resins and nanocomposites. Journal of Polymers and the Environment. 2013;21(3):658-74. https://doi.org/10.1007/s10924-013-0584-0
9. Abdurrahmanoglu S, Can V, Okay O. Design of high-toughness polyacrylamide hydrogels by hydrophobic modification. Polymer. 2009;50(23):5449-55. https://doi.org/10.1016/j.polymer.2009.09.042
10. Abass KH, Hamed A. Reduction of Energy Gap in ZrO2 Nanoparticles on Structural and Optical Properties of Casted PVA–PAAm Blend. Journal of Green Engineering. 2020;10(7):4166-76.
11. Zhan Y, Lu Y, Peng C, Lou J. Solvothermal synthesis and mechanical characterization of single crystalline copper nanorings. Journal of crystal growth. 2011;325(1):76-80. https://doi.org/10.1016/j.jcrysgro.2011.04.031
12. Cui F, Yu Y, Dou L, Sun J, Yang Q, Schildknecht C, Schierle-Arndt K, Yang P. Synthesis of ultrathin copper nanowires using tris (trimethylsilyl) silane for high-performance and low-haze transparent conductors. Nano letters. 2015;15(11):7610-5. https://doi.org/10.1021/acs.nanolett.5b03422
13. Han S, Hong S, Ham J, Yeo J, Lee J, Kang B, Lee P, Kwon J, Lee SS, Yang MY. Fast plasmonic laser nanowelding for a Cu-nanowire percolation network for flexible transparent conductors and stretchable electronics. Advanced materials. 2014;26(33):5808-14. https://doi.org/10.1002/adma.201400474
14. Al Asadi SM, Hamood FJ, Abass KH, Mohammed SK, Hassan IM, Latif DM. The Effect of MGO Nanoparticles on Structure and optical Properties of PVA-PAAm Blend. Research Journal of Pharmacy and Technology. 2019;12(6):2768-71. https://doi.org/10.5958/0974-360X.2019.00464.5
15. Yue YM, Xu K, Liu XG, Chen Q, Sheng X, Wang PX. Preparation and characterization of interpenetration polymer network films based on poly (vinyl alcohol) and poly (acrylic acid) for drug delivery. Journal of applied polymer science. 2008;108(6):3836-42. https://doi.org/10.1002/app.28023
16. Manjunath A, Deepa T, Supreetha NK, Irfan M. Studies on AC electrical conductivity and dielectric properties of PVA/NH 4 NO 3 solid polymer electrolyte films. Advances in Materials Physics and Chemistry. 2015;5(08):295. http://www.scirp.org/journal/PaperInformation.aspx?PaperID=58585&#abstract
17. Abdali K. Structural, Morphological, and Gamma Ray Shielding (GRS) Characterization of HVCMC/PVP/PEG Polymer Blend Encapsulated with Silicon Dioxide Nanoparticles. Silicon. 2022:1-6. https://doi.org/10.1007/s12633-022-01678-8
18. Deshmukh K, Ahmad J, Hägg MB. Fabrication and characterization of polymer blends consisting of cationic polyallylamine and anionic polyvinyl alcohol. Ionics. 2014;20(7):957-67. https://doi.org/10.1007/s11581-013-1062-3
19. Mansur HS, Sadahira CM, Souza AN, Mansur AA. FTIR spectroscopy characterization of poly (vinyl alcohol) hydrogel with different hydrolysis degree and chemically crosslinked with glutaraldehyde. Materials Science and Engineering: C. 2008;28(4):539-48. https://doi.org/10.1016/j.msec.2007.10.088
20. Dweik H, Sultan W, Sowwan M, Makharza S. Analysis characterization and some properties of polyacrylamide copper complexes. International Journal of Polymeric Materials. 2008;57(3):228-44. https://doi.org/10.1080/00914030701413280
21. Luo Y-L, Chen L-L, Xu F, Feng Q-S. Fabrication and characterization of copper nanoparticles in PVA/PAAm IPNs and swelling of the resulting nanocomposites. Metals and Materials International. 2012;18(5):899-908. https://doi.org/10.1007/s12540-012-5024-5
22. Dahshan M. Introduction to Material Science and engineering. 2nd, McGraw Hill, New York. 2002.
23. Al-jamal AN, Hadi QM, Hamood FJ, Abass KH, editors. Particle size effect of Sn on structure and optical properties of PVA-PEG blend. 2019 12th International Conference on Developments in eSystems Engineering (DeSE); 2019: IEEE. https://doi.org/10.1109/DeSE.2019.00137.
24. Abass KH, Shinen MH, Alkaim AF. Preparation of TiO2 nanolayers via sol-gel method and study the optoelectronic properties as solar cell application. Journal of Engineering and Applied Sciences. 2018;13(22):9631-7.
25. Abass KH, Adil A, Mohammed MK. Fabrication and enhancement of SnS: Ag/Si solar cell via thermal evaporation technique. Journal of Engineering and Applied Sciences. 2018;13(4):919-25.
26. Abass KH, Obaid NH, editors. 0.006 wt.% Ag-Doped Sb2O3 Nanofilms with Various Thickness: Morphological and optical properties. Journal of Physics: Conference Series; 2019: IOP Publishing. https://iopscience.iop.org/article/10.1088/1742-6596/1294/2/022005/meta
27. Atyia H. Influence of deposition temperature on the structural and optical properties of InSbSe~ 3 films. Journal of optoelectronics and advanced materials. 2006;8(4):1359. Available from: https://citeseerx.ist.psu.edu/messages/downloadsexceeded.html
28. Ahmed FS, Ahmed NY, Ali RS, Habubi NF, Abass KH, Chiad SS. Effects of substrate type on some optical and dispersion properties of sprayed CdO thin films. NeuroQuantology. 2020;18(3):56. Available from: https://uomustansiriyah.edu.iq/media/attachments/221/221_2020_06_04!05_35_27_AM.pdf
29. Abass KH, Latif D. The urbach energy and dispersion parameters dependence of substrate temperature of CdO thin films prepared by chemical spray pyrolysis. International Journal of ChemTech Research. 2016;9(9):332-8. Available from: https://www.researchgate.net/publication/309565096
30. Zbala AAK, Al-Ogaili AOM, Abass KH. Optical Properties and Dispersion Parameters of PAAm-PEG Polymer Blend Doped with Antimony (III) Oxide Nanoparticles. NeuroQuantology. 2022;20(2):62-9. Available from:

http://www.neuroquantology.com/index.php/journal